J Mater Sci (2009) 44:6149–6154
DOI 10.1007/s10853-009-3850-8

Effect of grain size and Cu-rich phase on the electric properties of $CaCu_3Ti_4O_{12}$ ceramics

Tao Li · Zhenping Chen · Yuling Su · Lei Su · Jincang Zhang

Received: 25 May 2009 / Accepted: 25 August 2009 / Published online: 4 September 2009
© Springer Science+Business Media, LLC 2009

Abstract The $CaCu_3Ti_4O_{12}$ ceramics were prepared by the traditional solid-state reaction method under different sintering conditions. The XRD patterns show that crystal structures of the samples are basically single-phase pseudo-cubic, except little second phases of CuO and Cu_2O in the samples sintered in air at 1050 and 1100 °C, respectively, for 12 h. The SEM results indicate that the pellet sintered at 1100 °C for 12 h possess larger grain size and more Cu-rich phases at the grain boundaries than the pellet sintered at 1050 °C for 12 h. It is interesting that the pellet sintered at 1050 °C under the pressure of 5 Gpa for 3 h shows smaller grain size ($\sim$1 μm) and no Cu-rich phases due to the higher pressure during the sintering process. The results show that the grain size has a reverse effect on the values of the permittivity and the values of breakdown electric field (E_b) and nonlinear coefficient. The pellet sintered at 1100 °C for 12 h exhibits a higher permittivity, but with a lower breakdown electric field (E_b) and a lower nonlinear coefficient due to larger grain size. The pellet sintered at 1050 °C under the pressure of 5 Gpa for 3 h exhibits a lower permittivity, but with a higher breakdown electric field (E_b) and a higher nonlinear coefficient due to smaller grain size. The Cu-rich phases at grain boundaries can raise the resistance of the grain boundary leading to the lower dielectric loss tangent, which has been supported by the results of impedance spectroscopy analysis.

T. Li (✉) · Z. Chen · Y. Su · L. Su · J. Zhang
Department of Technology and Physics, Zhengzhou University of Light Industry, 450002 Zhengzhou, People's Republic of China
e-mail: hnlt529@126.com

Introduction

Electroceramics with excellent performance have drawn more and more attention for their potential application in miniaturized electronic components/devices. Recently, an unusual cubic perovskite material $CaCu_3Ti_4O_{12}$ (CCTO) has attracted much attention owing to its high dielectric permittivity ($\sim 10^4$–10^5) by low loss at low frequencies at room temperature and its good stability over a wide temperature range from 100 to 600 K [1–3]. Structural studies have showed that CCTO maintains a body-centered cubic structure with the space group *Im*3 without any phase transitions down to 35 K [1, 4]. Despite many attempts, including theoretical calculations, have been performed to explain the nature and origin of the giant dielectric constant of CCTO ceramic, its nature and origin still remain unclear to date. At present, a plausible explanation accepted widely is the internal barrier layer capacitors (IBLC) model at the grain boundaries between semiconducting grains [4–6]. In addition, some other explanations reported are also worthy paying attention to, such as bimodal grain size model [7], internal domain [8], electrode polarization effect [8], Cu-stoichiometry effect [9], and so on. However, it can be convinced that more and more effective evidence will be provided to reveal the true reasons.

In addition to the intriguing dielectric property, the non-ohmic behavior of CCTO is also interesting and more and more attention is being attracted. In 2004, Chung et al. [10] found that the nonlinear coefficient (α) of CCTO ceramics reaches the value of 912 when measured in the range of 5–100 mA. Recently, Marques et al. [11] and Dun-Lu Sun et al. [12] both have reported the excellent nonohmic behavior of CCTO ceramics. In the past, the research on the varistors mainly centered around $SrTiO_3$- and ZnO-based materials. With the development of automatic control and

semiconductor circuits, the higher demand has been proposed for the performance of varistors. ZnO-based material can not meet this requirement because its breakdown voltage is too high; neither can $SrTiO_3$-based material, because its surface layer structure makes it hard to improve the breakdown voltage. However, the breakdown voltage of CCTO ceramics can be changed through the preparation techniques. Therefore, CCTO ceramics are considered as a very promising material for application in microelectronics, especially in capacitive components and varistors.

In this article, the CCTO ceramics are prepared using traditional solid-state reaction method. The influence of grain size and Cu-rich phase on the dielectric property and the nonohmic property of the CCTO ceramics has been analyzed and discussed.

Experimental procedure

The single-phase CCTO polycrystalline powder was prepared by the traditional solid-state reaction method. All the raw materials used were analytical grade: $CaCO_3$ (>99.5%), CuO (>99.6%), TiO_2 (>99.8%). First, the raw materials were weighed out in the proportion of 1:3:4, ball-milled in alcohol for 12 h, dried, and then calcined at 950 °C for 12 h. The calcined powder was remilled for 2 h again to eliminate the agglomerates and granulated by adding PVA, then pressed into pellets (150 MPa) with a diameter of 12.0 mm and thickness of 2.0 mm. Next, sample1# and sample2# were sintered in air at 1050 and 1100 °C, respectively, for 12 h. Sample3# was sintered in air at 1050 °C under the pressure of 5 Gpa for 3 h. Finally, the obtained pellets were subjected to a thermal treatment in air at 800 °C for 2 h. In order to measure the electric properties, silver paste was painted on the polished samples as the electrodes and fired at 600 °C for 15 min.

Microstructural characterization of the pellets was carried out in a scanning electron microscope (SEM) at 15 kV, with the samples coated by a Pd–Au film. X-ray diffraction (XRD) with Cu K radiation ($\lambda = 0.1541$ nm) was performed to examine the phase constitution of specimens at room temperature. The permittivity (ε_r) and loss tangent ($\tan\delta$) and the complex impedance of the samples were determined using an Agilent 4294A Precision Impedance Analyzer from 40 Hz to 110 MHz. The current–voltage (*I–V* or *J–E*) characteristics were measured by using a high voltage measuring unit (Trek model 609B) while the varistors were put into silicon oil. It is important to emphasize that the nonlinear coefficient (α) values were calculated in terms of the following formula: $\alpha = \frac{\lg(I_2 I_1)}{\lg(V_2 V_1)}$. Where V_1 and V_2 are, respectively, the voltage at current I_1 and I_2, α is calculated when $I_1 = 1$ mA, $I_2 = 10$ mA, respectively. The breakdown electric field (threshold electric field) (E_b) is obtained when a current density of 1 mA flowing through the varistors.

Results and discussions

SEM and X-ray diffraction analysis

The densities of the sintered pellets were measured using the Archimedes method. The relative density for samples 1#, 2#, and 3# is 92.3, 94.9 and 90.3%, respectively (the theoretical density of CCTO is 4.9 g/cm^3 [13]).

The SEM pictures of the microstructures of the specimens under different sintering conditions are shown in Fig. 1. The micrograph of the CCTO pellets sintered at 1050 °C for 12 h (Fig. 1, No.1#) shows that the mean grain size is about 8 ± 2 μm and the grain boundaries are filled with the light colored exfoliated sheets identified as Cu-rich phases (in the XRD patterns). The micrograph of those sintered at 1100 °C for 12 h (Fig. 1, No.2#) reveals that mean grain size is about 20 ± 5 μm and the grains are surrounded by melted Cu-rich phase, which is in agreement with the report [14, 15]. The micrograph of those sintered at 1050 °C under the pressure of 5 Gpa for 3 h shows that the grain size is about 1 μm, and the Cu-rich phase does not appear at the grain boundaries. The smaller grain size and disappearance of Cu-rich phase for sample3# may be attributed to the higher sintering pressure and shorter sintering duration. The SEM results indicate that the higher sintering temperature and longer sintering duration contribute to the growth of grains and the formation of Cu-rich phase under the normal pressure. The differences of the mean grain size and Cu-rich phases of the samples owing to the different sintering conditions may be sufficient to cause the differences in their electric properties.

The XRD powder pattern obtained for the specimens is shown in Fig. 2a, b. All the major diffraction peaks of samples 1#, 2#, and 3# are matched with the peaks of the pseudo-cubic CCTO by comparing with the standard PDF database [JCPDF File No. 75-2188], except two weak peaks of the second phases of CuO (around 35.5°) and Cu_2O (near 36.5°) are present in the amplified XRD patterns (Fig. 2b) of samples 1# and 2# comparing with that of sample3#, which confirms the above discussion of SEM. The results calculated using Powder X program indicate that crystal structure is cubic and the lattice parameters are 7.392, 7.394, and 7.389 Å corresponding to sample1#, sample2#, and sample3#, respectively.

Dielectric properties analysis

The frequency dependence of permittivity and dielectric loss at room temperature of the specimens under different

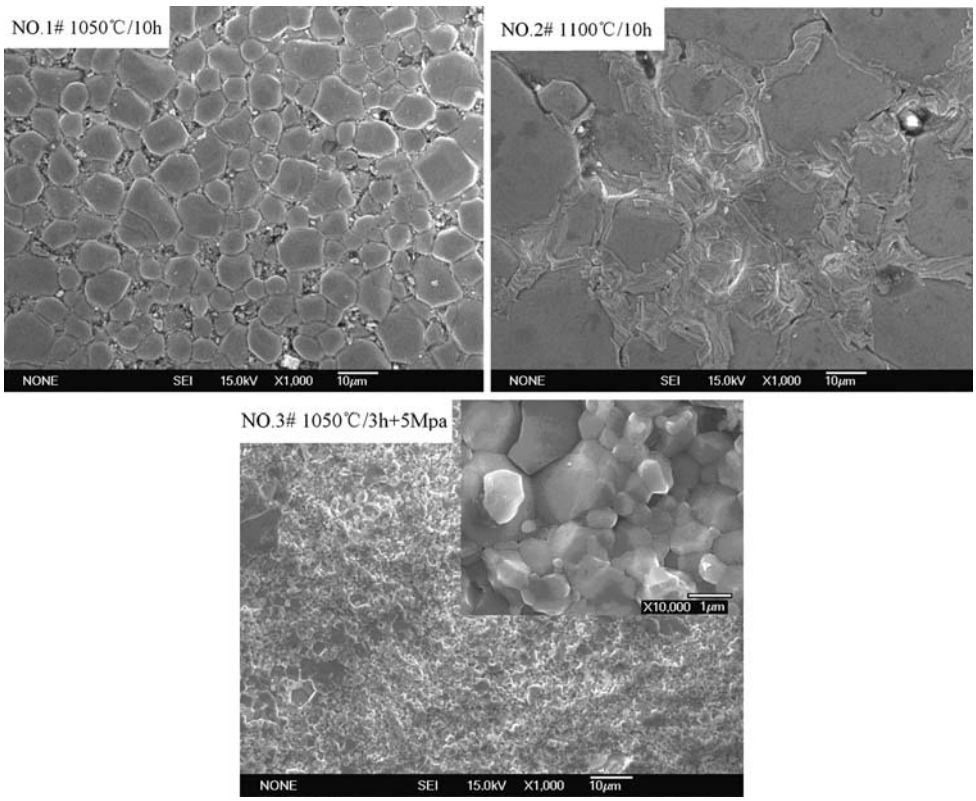

Fig. 1 SEM pictures the CCTO samples under different sintering conditions

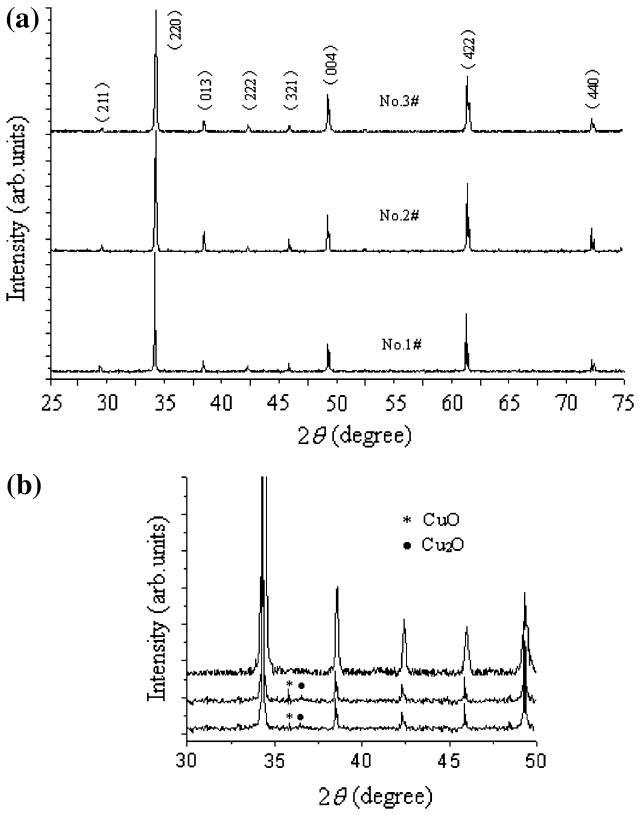

Fig. 2 **a** XRD patterns of the CCTO samples under different sintering conditions. **b** The amplified XRD patterns of the CCTO samples under different sintering conditions

sintering conditions is given in Fig. 3a, b. It can be found that all the samples show giant permittivity of $\varepsilon_r > 7000$ below 1 MHz and each curve presents a more stable plateau in a broad frequency range followed by a strong drop for about 1 GHz as previously reported [3, 9]. The permittivity increases with the growth of the grain size. The permittivity of the sample2# is largest, which is about 1.5 times that of sample1# and more than 3 times that of sample3# below 1 MHz. The frequency dependence of dielectric loss tangent (tanδ) of the samples is shown in Fig. 3b and the tangent at below 10^6 Hz is also given as an inset. It can be found that tanδ of sample2# is smaller than that of samples 1# and 3# at low frequency. Dielectric loss tangent is obviously frequency dependence and begins to increase quickly above 10^6 Hz for all samples. Debye relaxations are observed at near 1 GHz as reported [16]. The values of ε_r and tanδ of the samples at selected frequencies are listed in Table 1.

The dielectric behaviors can be explained by the IBLC model which is assumed that the grain and grain boundary form a two-layer capacitor with a thickness ($d_g + d_{gb}$). Where d_g and d_{gb} are the mean grain size and the width of the grain boundary layer, respectively. The effective dielectric constant (ε_{eff}) of such a unit of IBLC can be estimated as: $\varepsilon_{eff} = \frac{d_g + d_{gb}}{d_{gb}} \varepsilon_{gb}$ [14]. Where ε_{gb} is the permittivity of insulating grain boundary layer. If the ratio of $(d_g + d_{gb})/d_{gb}$ is large, it can lead to a giant ε_{eff} even a small ε_{gb}. So the permittivity (ε_r) is highly dependent upon

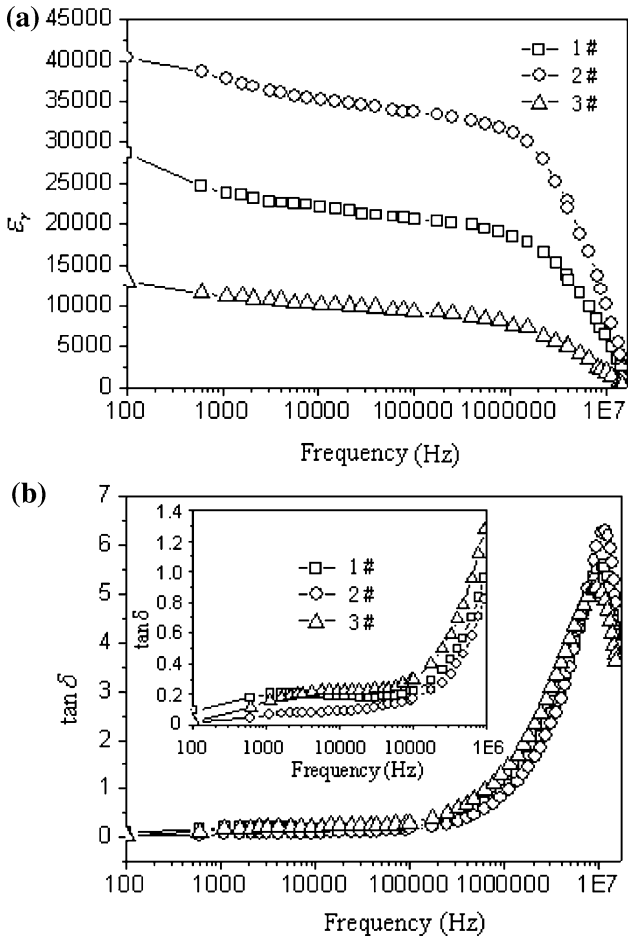

Fig. 3 Frequency dependence of permittivity (**a**) and loss (**b**) of the CCTO samples under different sintering conditions

the grain size and the thicknesses of the grain boundary layer. The grain size has been obtained from SEM pictures, being about 20 mm for the sample2#, which is about 2.5 times larger than that of sample1# (8 μm) and about 20 times larger than that of sample3# (1 μm). In addition, considering the relative density for samples obtained in the above, the sample2# has a smaller volume fraction taken up by grain boundary layers than sample1# and so does the latter than sample3#. This indicates that sample2# has the thinner d_{gb} than sample1# and so does the latter than sample3#. So it is easy to understand why the permittivity (ε_r) of sample2# is much larger than that of sample1#, and so is the latter than that of sample3#. In addition, as substance of dielectric insulator, the Cu-rich phase existing at the grain boundary is also contributing to the increase of the permittivity and the reduction of the dielectric loss. Sample2# possesses the largest permittivity and the lowest dielectric loss. This partly can be attributed to for much Cu-rich at the grain boundary which leads to the largest resistance of a unit IBLC in the materials.

Nonohmic characteristic

Figure 4 shows the nonlinear (J–E) characteristic at room temperature for the specimens. A strong nonlinear relationship between J and E is observed for all the samples. The breakdown electric field (E_b) of samples 1#, 2#, and 3# is 0.59, 0.36, and 0.92 kv/cm which correspond to the voltage of 118, 72, and 184 V, respectively. Based on the formula described above, the value of coefficient $\alpha = 8.7$ for sample1#, $\alpha = 6.4$ for sample2#, and $\alpha = 10.5$ for sample3# has been obtained at room temperature. The experimental results are better than those reported in the literature [11, 17]. It can be found that α and E_b increase, just have a reverse behaviors with the permittivity when grain size decreases. The sample3# has a low permittivity, but its nonlinear coefficient and breakdown electric field are higher than that of other samples.

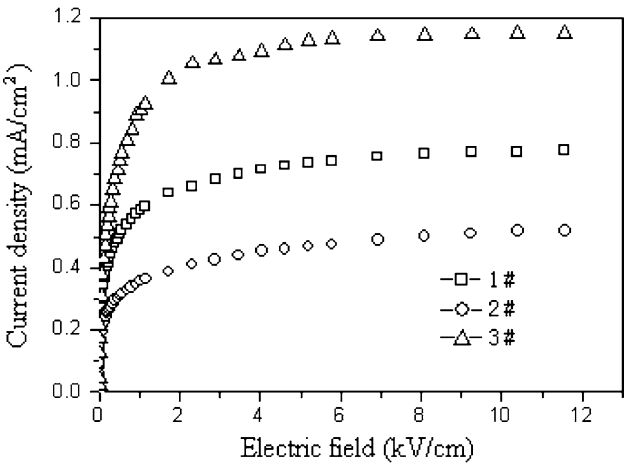

Fig. 4 Nonlinear current–voltage behaviors of the CCTO samples under different sintering conditions

Table 1 The values of ε_r and tanδ of the CCTO samples at selected frequencies

Samples	100 Hz		1 kHz		10 kHz		100 kHz		1 MHz	
	ε_r	tanδ	ε_r	tanδ	ε_r	tanδ	ε_r	tanδ	ε_r	tanδ
#1	28,700	0.094	24,000	0.20	22,200	0.18	20,500	0.22	18,900	1.02
#2	40,300	0.028	38,000	0.071	35,200	0.089	33,800	0.21	31,600	1.19
#3	13,000	0.027	11,400	0.15	10,200	0.22	9,200	0.30	7,900	1.35

During the sintering process, the cation Cu^{2+} or Cu^{+} released from Cu-rich phases and the oxygen atoms from air entering the grain boundary, as acceptors, can raise the concentration of acceptor and enhance the height of Schottky barriers at the grain boundaries. The effect of Schottky barriers at grain boundaries on the *I–V* behavior can be described in terms of the following equation [12]:

$$J = AT^2 \exp[(\beta E^{1/2} - \Phi_B)/k_B T] \quad (1)$$

where A is Richardson's constant, Φ_B is the height of Schottky barriers, k_B is the Boltzman constant, β is a constant related to the potential barrier width, and T is the temperature (K). According to the Eq. 1, the obtained values of Φ_B for samples 1#, 2#, and 3# are 0.86, 0.88, and 0.82 eV, respectively. The values are close to the reported barrier height of 0.79–0.90 eV [18]. The calculated values of Φ_B indicate that the higher Φ_B, the higher resistance of a unit IBLC. Nevertheless, the effect of Schottky barrier height on the breakdown voltage is weak for its inconspicuous variations roughly considered the same, comparing with that of grain size on the samples. The breakdown voltage, V_S, can be thought roughly proportional to the mean number of barriers $\bar{N}$ [19].

$$V_S = \bar{N} \cdot v_b \quad (2)$$

where v_b is the barrier voltage at the grain boundary. If the thickness of pellets is same, the reduction of the mean grain size means the increase of the number of boundary barriers. So, it is easy to understand why the breakdown electric field (E_b) of sample3# has the highest value, that of sample2# has the lowest value, and that of sample1# has an intermediate value. The coefficient has the similar change trend with the breakdown electric field for the samples, which indicates that the coefficient is also affected by the grain size. This phenomenon is due to the grain size having a reverse effect on the values of the permittivity and the values of breakdown electric field (E_b) and nonlinear coefficient.

High nonlinear coefficient is suitable for the application of varistor, switching, and gas-sensing devices [12]. The different sintering conditions have different influence on the dielectric properties and the varistor properties. Therefore, a suitable sintering condition can be selected to adjust the permittivity and *I–V* nonlinearity according to different desired device applications.

Impedance spectroscopy study

The impedance of electroceramics has been modeled as an equivalent circuit consisting of two parallel RC elements connected in series, of which one RC element is for the semi-conductive bulk contribution and the other is for the grain boundary response [20]. An impedance complex, Z^*, plane diagram plot obtained should consist of two semicircular arcs. The large one is due to the grain boundary responses at low frequencies, and the small one is due to the bulk grain responses at high frequencies. In actual measurements, it is hard to obtain both semicircular arcs in one Z^* plot, especially for the small one associated with the bulk grains. So, the nonzero intercept of large arc at high frequencies usually represents the resistance of grains (R_g) and that at low frequency represents the resistance of grains boundary (R_{gb}). Figure 5 shows the Z^* (Z' vs. $-Z''$) plots and the curve fits for the samples at room temperature. It has been found that Z' intercepts of sample2# is 2790 kΩ cm at low frequencies, but that of samples 1# and 3# are too large to show in the Fig. 5. However, in terms of the curvature radius of Z^* curve fits, it can be concluded that the relation of the Z' intercepts of curve fits of samples is $R_{gb3\#} > R_{gb1\#} > R_{gb2\#}$. This is because smaller grain size leads to more number of barriers in materials. The large R_{gb} is often indicative of high breakdown voltage for the varistor. The inset of the detailed trend of nonzero resistances at the maximum frequency shows that the approximate resistance values of samples 1#, 2#, and 3# at high frequency are 78.5, 62.1, and 87.2 Ω cm, respectively, which indicates that the reduction of grain size results in the increase of the R_g of the samples at high frequency.

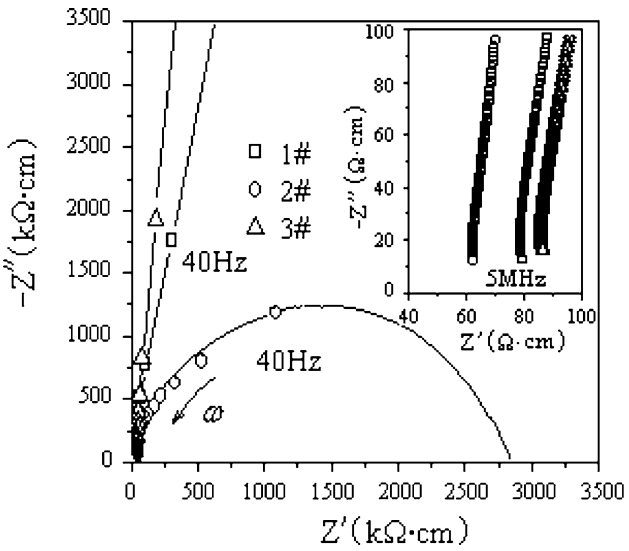

Fig. 5 Impedance complex plane plots and the curve fits of the CCTO samples sintered under different conditions

Conclusions

The microstructures observed by SEM in CCTO ceramics show that the longer sintering duration and higher sintering temperature under the normal pressure are conducive to the growth of grain and the formation of Cu-rich phase at the

grain boundary. Shorter sintering duration and higher pressure during the sintering progress can hinder the growth of crystal grains, and can also deter the formation of Cu-rich phase. The more Cu-rich phases at the grain boundary result in the higher Schottky barrier height. The electric properties measurement show that the pellet sintered at 1100 °C for 12 h with the largest grain size, more Cu-rich phases at the grain boundary exhibits the largest permittivity and the smallest dielectric loss tangent, but the lowest nonlinear coefficient and breakdown voltage. However, the pellet sintered at 1050 °C under the press of 5 Gpa for 3 h exhibits the largest nonlinear coefficient and breakdown voltage, but the lowest permittivity. The impedance spectroscopy analysis can well support these view points.

Acknowledgements This study is supported by National Natural Science Foundation of China (Project No. 10875107), The Natural Science Foundation of Henan (No. 082300440080), and The Basic Research Plan on Natural Science of the Education Department of Henan Province (Grant No. 2008A140014).

References

1. Ramirez AP, Subramanian MA, Gardel M, Blumberg G, Li D, Vogt T, Shapiro SM (2000) Solid State Commun 115:217
2. Homes CC, Vogt T, Shapiro SM, Wakimoto S, Ramirez AP (2001) Science 293:673
3. Brizé V, Gruener G, Wolfman J, Fatyeyeva K, Tabellout M, Gervais M, Gervais F (2006) Mater Sci Eng B 129:135
4. Subramanian MA, Sleight AW (2002) Solid State Sci 4:347
5. West AR, Adams TB, Morrison FD, Sinclair DC (2004) J Eur Ceram Soc 24:1439
6. Grubbs RK, Venturini EL, Clem PG, Richardson JJ, Tuttle BA, Samara GA (2005) Phys Rev B 72:104111
7. Pan MJ, Bender BA (2005) J Am Ceram Soc 88(9):2611
8. Fang T-T, Liu CP (2005) Chem Mater 17:5167
9. Shao SF, Zhang JL, Zheng P, Wang CL (2007) Solid State Commun 142:281
10. Chung S, Kim ID, Kang SJL (2004) Nat Mater 3:774
11. Marques VPB, Ries A, Simoes AZ, Ramirez MA, Varela JA, Longo E (2007) Ceram Int 33:1187
12. Sun D-L, Wu A-Y, Yin S-T (2008) J Am Ceram Soc 91(1):169
13. Ranabrata M, Anshuman S, Amarnath S, Himadri SE (2005) Ferroelectrics 326:103
14. Shri Prakash B, Varma KBR (2006) Physica B 382:312
15. Hutagalung SD, Ooi LY, Ahmad ZA (2009) J Alloy Compd 476:477
16. Mu C-H, Liu P, He Y, Zhou J-P, Zhang H-W (2009) J Alloy Compd 471:137
17. Leret P, Fernandez JF, de Frutos J, Fernández-Hevia D (2007) J Eur Ceram Soc 27:3901
18. Zang GZ, Zhang JL, Zheng P, Wang JF, Wang CL (2005) J Phys D 38(11):1824
19. Wang JF, Chen HC, Su WB, Zang GZ, Zhang CJ, Wang CM, Qi P (2005) J Electroceram 14:133
20. Sinclair DC, Adams TB, Morrison FD, West AR (2002) Appl Phys Lett 80:2153